Journal of Molecular Catalysis A: Chemical 323 (2010) 91–100

Contents lists available at ScienceDirect

Journal of Molecular Catalysis A: Chemical

journal homepage: www.elsevier.com/locate/molcata

Theoretical study on the mechanisms of the conversion of methyl lactate over sodium polyphosphate catalyst

Zhiqiang Zhang[b], Yixin Qu[a], Shui Wang[a], Jidong Wang[a,*]

[a] Beijing Key Laboratory of Bioprocess, College of Chemical Engineering, Beijing University of Chemical Technology, Beisanhuan East Road 15, Chaoyang District, Beijing 100029, PR China
[b] College of Mining Engineering, Taiyuan University of Technology, Taiyuan 030024, PR China

ARTICLE INFO

Article history:
Received 25 October 2009
Received in revised form 22 March 2010
Accepted 23 March 2010
Available online 30 March 2010

Keywords:
Methyl lactate
Conversion
Sodium polyphosphate
Quantum mechanical calculation

ABSTRACT

The conversion of methyl lactate (ML) over sodium tripolyphosphate, a model catalyst derived from silica supported sodium polyphosphate, was studied systematically by quantum mechanical calculations using MP2 and B3LYP methods. The reaction profiles of ML and its reaction products, acrylic acid (AA), methyl acrylate (MA) and lactic acid (LA) via various reactions such as dehydration, decomposition, decarbonylation, hydrolysis and esterification has been determined with the catalyst. For each reaction, the intermediate and transition state as well as their energetics were calculated. Over the catalyst, the main consumption routes for ML were identified to be the direct decomposition to AA and methanol and decarbonylation to acetaldehyde (AD), methanol and carbon monoxide. Both of the above reactions start from the same reaction intermediate. The main route for the formation of MA was supposed to be via esterification of AA with methanol. The values of activation barriers also indicate that over the sodium polyphosphate catalyst conversion of ML to AA has a higher selectivity than that from LA to AA.

1. Introduction

The continuous rising of oil price lets one to explore new ways to manufacture chemicals with renewable resources. As a consequence, techniques for the production of chemicals from biomass attract more attention recently [1–3]. At present, the main methods to convert biomass to chemicals are various fermentation processes. Among these, fermentation of biomass to LA is the most effective one. The capacity of LA via fermentation in the world amounts to 120,000 t y^{-1} [2]. Therefore, processes based on LA or its derivatives to produce chemicals have been proposed [3]. One of them is the dehydration of LA to AA or dehydration of LA esters to AA and acrylates, which are widely used in the chemical industry.

Dehydration of LA or its esters is carried out in gas phase in the presence of a catalyst. The catalysts which have been investigated for these reactions mainly include sulfate [4], phosphate [5] mixtures of sulfate and phosphate [4,6,7] and Y-zeolite modified with alkali or rare earth metals [8–10]. The dehydration of ML over H_3PO_4 and sodium phosphates supported on silica has been investigated recently by us [11,12]. It was found that the selectivity of ML to acrylates (MA + AA) on silica supported NaH_2PO_4 was higher than that on the supported H_3PO_4 and other sodium phosphates. The best selectivity of 52 mol% (MA + AA) was observed for silica supported NaH_2PO_4 with a conversion of ML close to 100%. Based on the results of catalyst characterization, it was proposed that the active sites on this catalyst was most likely the terminal POH groups of sodium polyphosphate chains which were produced upon the calcinations of silica supported NaH_2PO_4.

The high boiling point and instability of LA make it an unsuitable feedstock for gas phase reaction since at elevated temperature LA easily polymerizes to high molecular products other than converts to desired products. An alternative way is to use esters of LA, such as ML as a feedstock, which is easily vaporized and more stable as compared to LA. It is expected that a higher selectivity to acrylates (MA + AA) would be obtained by using ML as a feedstock than by using LA. This has been conformed by our recent study with silica supported NaH_2PO_4 as catalysts. With a conversion close to 100%, the selectivity to AA from LA is only 26%, which was significantly lower than 52% (MA + AA) obtained from ML [11].

In addition to dehydration, ML can also undergo decarbonylation to give AD, methanol and CO as well as decarboxylation to AD, methane and CO_2. The selectivity from the conversion of ML to various products depends on the competition between dehydration, decarbonylation and decarboxylation over the catalysts. At present, the reported selectivity from LA or ML to acrylates is generally less than 70%, which is still under the levels that are commercially inter-

Abbreviations: ML, methyl lactate; AA, acrylic acid; MA, methyl acrylate; LA, lactic acid; AD, acetaldehyde; STQN, synchronous transit-guided quasi-Newton; IRC, intrinsic reaction coordinate.

* Corresponding author. Tel.: +86 10 6443 4785; fax: +86 10 6443 6781.
E-mail addresses: jidongwang1963@yahoo.com.cn, yangmou@126.com (J. Wang).

1381-1169/$ – see front matter © 2010 Elsevier B.V. All rights reserved.
doi:10.1016/j.molcata.2010.03.027

esting. Therefore, further improvement of the catalysts is necessary and understanding of the reaction mechanisms on various catalysts is helpful for this purpose.

In this paper, the conversion of ML and LA over a model catalyst, which was derived based on the silica supported NaH_2PO_4, was investigated using quantum chemical calculations. Based on the calculation results, the main conversion routes of ML and LA over the catalyst were identified and the selectivity to various products was explained.

2. Computational details

2.1. Reactions

The main chemical reactions involved in the conversion of ML over sodium polyphosphate include [11]:

$$CH_3CH(OH)COOCH_3(ML) \rightarrow CH_2{=}CHCOOCH_3(MA) + H_2O \quad (1)$$

$$CH_3CH(OH)COOCH_3(ML) \rightarrow CH_3CHO(AD) + CH_3OH + CO \quad (2)$$

$$CH_3CH(OH)COOCH_3(ML) \rightarrow CH_2{=}CHCOOH(AA) + CH_3OH \quad (3)$$

$$CH_3CH(OH)COOCH_3(ML) + H_2O \rightarrow CH_3CH(OH)COOH(LA) + CH_3OH \quad (4)$$

$$CH_3CH(OH)COOH(LA) + CH_3OH \rightarrow CH_3CH(OH)COOCH_3(ML) + H_2O \quad (5)$$

$$CH_2{=}CHCOOCH_3(MA) + H_2O \rightarrow CH_2{=}CHCOOH(AA) + CH_3OH \quad (6)$$

$$CH_2{=}CHCOOH(AA) + CH_3OH \rightarrow CH_2{=}CHCOOCH_3(MA) + H_2O \quad (7)$$

$$CH_3CH(OH)COOH(LA) \rightarrow CH_2{=}CHCOOH(AA) + H_2O \quad (8)$$

$$CH_3CH(OH)COOH(LA) \rightarrow CH_3CHO(AD) + H_2O + CO \quad (9)$$

$$CH_3CH(OH)COOCH_3(ML) \rightarrow CH_3CHO(AD) + CH_4 + CO_2 \quad (10)$$

$$CH_3CH(OH)COOH(LA) \rightarrow CH_3CHO(AD) + H_2 + CO_2 \quad (11)$$

Reaction (1) is the dehydration of ML to MA and H_2O. Reaction (2) is the decarbonylation of ML to AD, methanol, and CO. In reaction (3) direct decomposition of ML gives AA and methanol. Due to the presence of H_2O and methanol in the reaction system, ML can be hydrolyzed to LA and methanol as shown in reaction (4) and the reverse reaction can also take place as shown in reaction (5). MA derived from ML can undergo similar reactions as reactions (4) and (5), which are presented in reactions (6) and (7). LA derived from ML can dehydrate to AA and H_2O as shown in reaction (8). It can also undergo decarbonylation, giving AD, H_2O and CO as shown in reaction (9). Reactions (10) and (11) are the decarboxylation of ML and LA. Since these two reactions are less important as compared to the other reactions, especially at lower temperature [11,12], they are not considered in this paper.

2.2. Model of catalyst

Results of the catalysts characterization indicated that sodium phosphate supported on silica was converted to polyphosphate chains upon calcination at temperature of 450 °C [11,12]. The structure of the sodium polyphosphate chains is shown in Fig. 1a. The chains contain [PO_3Na] units in their middle part and [HO–PO_2Na] units at their ends. Based on this structure, it can be imagined that the shortest polyphosphate chain is sodium tripolyphosphate as shown in Fig. 1b. It has one [PO_3Na] unit in the middle and two [HO–PO_2Na] units at its ends. To simplify the calculations, sodium tripolyphosphate was selected as a model of the sodium polyphosphate catalyst.

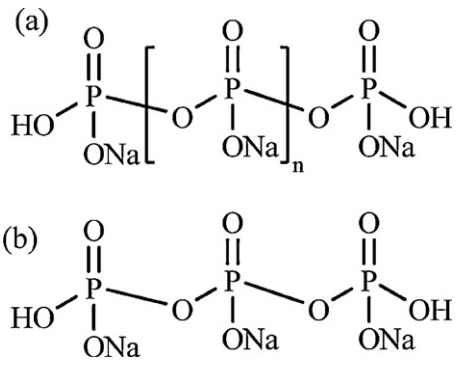

Fig. 1. Chemical structure of (a) sodium polyphosphate and (b) sodium tripolyphosphate.

2.3. Calculation method

For the purpose of searching for the most favorable reaction pathways, equilibrium and transition structure of the reactions (1)–(9) over the model catalyst were theoretically determined using quantum mechanical calculations. The calculations were performed with Gaussian 03 package [13]. The stationary points on the reaction potential energy surfaces were optimized on the computational level of B3LYP/6-31+G (d,p), and analytical harmonic vibration frequencies were computed at the same level to character the located stationary points: one imaginary frequency for a transition state and all real frequencies for a minimum. The transition states were optimized by using synchronous transit-guided quasi-Newton (STQN) method. This method, implemented by Schlegel and co-workers [14,15], uses a quadratic synchronous transit approach to get closer to the quadratic region of the transition state and then uses a quasi-Newton or eigenvector-following algorithm to complete the optimization. The relation between the transition states and the corresponding minima was verified by performing intrinsic reaction coordinate (IRC) calculations [16]. In this study the energetics were estimated at the B3LYP/6-31+G (d,p) and MP2/6-31+G (d,p) levels using the B3LYP/6-31+G (d,p) optimized structures. In the following text, both of them are presented with the values obtained at the B3LYP/6-31+G (d,p) level being given in the parentheses.

3. Results and discussion

The presence of the hydroxyl groups at the terminals of the sodium polyphosphate renders the catalyst having Brønsted acidity. These terminal [HO–PO_2Na] units are supposed to be the active sites for the conversion of ML [11,12]. In the catalytic process, proton transfer involved between the reaction molecules and the active sites is supposed to be confined to the terminal POH and P=O groups of the terminal [HO–PO_2Na] units. Proton transfer from the terminal POH groups to the P=O groups belonging to the middle [PO_3Na] units seems impossible since this needs migration of the Na^+ cations from the middle sites to the end sites in order to keep the terminal phosphorus atoms at +5 valence state. In addition, proton transfer from the terminal POH groups to the P=O groups belonging to the middle [PO_3Na] units would result in the forma-

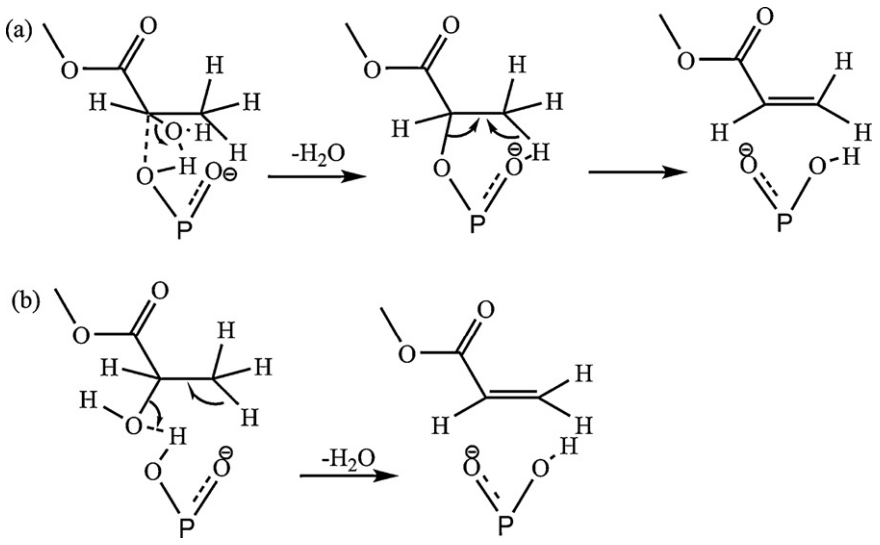

Fig. 2. Schematic reaction mechanisms of the gas phase dehydration of ML over the sodium polyphosphate catalyst. (a) stepwise mechanism; (b) concerted mechanism.

tion of P–OH groups that have a stronger acidity (pK_a = 2.12) than that of the terminal P–OH groups (pK_a = 8.0) [17,18]. The possibility for such a process to occur seems very small.

In order to elucidate the catalytic effect of the active sites, schematic reaction mechanisms for the dehydration of ML to MA via a stepwise and a concerted dehydration route over the catalyst are shown in Fig. 2. In the stepwise route, the acid site induces the abstraction of the hydroxyl group of ML via donating a proton. Then proton relay completes via water molecule releasing and "alkoxide" formation. The "alkoxide" further donates one proton to the P═O group and dissociates from the catalyst surface, which regenerates the active site and leads to the formation of MA. In the concerted route, elimination of H_2O via the α-hydroxyl group of ML and the proton of P–OH and donation of a β-hydrogen of ML to the P═O group occurs at the same time, resulting in the formation of MA and regeneration of the active site. Detailed reaction mechanisms will be seen in the following sections.

3.1. Dehydration of ML to MA

The dehydration mechanisms of ML to MA over the model catalyst are shown in Fig. 3. Two stepwise mechanisms (Fig. 3a and b) and a concerted mechanism (Fig. 3d) are proposed. The two stepwise mechanisms involve the formation of an intermediate of phosphate ester which is produced via the reaction of ML with the POH group of the catalyst. In Fig. 3a, the phosphate ester (P1) is produced via elimination of the hydroxyl group of ML and the proton of POH with an activation barrier of 398 (398) kJ mol^{-1}. In Fig. 3b the phosphate ester (P2) is produced via elimination of the proton of the hydroxyl group of ML and the hydroxyl of POH group of the catalyst with an activation barrier of 219 (221) kJ mol^{-1}. Upon changing their conformations, P1 and P2 convert to R3, which then decomposes by transfer of a proton from the methyl group of ML to P═O and break of the C–O bond to MA with an activation barrier of 222 (193) kJ mol^{-1} The concerted mechanism from ML to MA is shown in Fig. 4d. In this mechanism the phosphate provides an acidic site to attack the hydroxyl group of ML and a basic site to abstract a proton from ML. The activation barrier of this reaction is 237 (203) kJ mol^{-1}. The calculated activation barriers for the dehydration of ML to MA indicate that at the MP2/6-31+G (d,p) level the stepwise mechanism shown in Fig. 3b and c and the concerted mechanism shown in Fig. 3d is the predominant pathways for the dehydration of ML with the former being favored over the latter, whereas at the B3LYP/6-31+G (d,p) level the concerted mechanism shown in Fig. 3d is more favorable than the stepwise mechanism.

3.2. Decarbonylation of ML

Decarbonylation of ML gives AD, methanol and CO. For this reaction, two possibilities were explored. The first one (Fig. 4a and b) is a stepwise mechanism, the second one (Fig. 4c) is a concerted mechanism. The first step of the stepwise decarbonylation (Fig. 4a) of ML on the catalyst can be regarded as a transesterification reaction between ML and the POH group of the catalyst, which acts like an alcohol. In the second stage (Fig. 4b), the reaction intermediate P5 converts to R6 via desorption of a methanol. R6 then decomposes to AD and CO via transfer of a proton from the hydroxyl group of ML to the P═O group of the catalyst and cleavage of a C–C bond and a C–O bond. For the stepwise decarbonylation of ML, the activation barrier of the first step is 160 (171) kJ mol^{-1}, which is higher than that of the second step, 155 (142) kJ mol^{-1}. The concerted mechanism for the decarbonylation of ML (Fig. 4c) involves a proton transfer from the POH to ML and a proton transfer from the hydroxyl group of ML to the P═O group of the catalyst and simultaneous cleavage of a C–C bond and a C–O bond. At the MP2/6-31+G (d,p) level, the activation barrier for the concerted decarbonylation of ML is 188 kJ mol^{-1}, which is 28 kJ mol^{-1} higher than that of the rate-determining step of the stepwise decarbonylation of ML. As a consequence, decarbonylation of ML over the catalyst can be regarded as to proceed mainly via the stepwise mechanism. However, at the B3LYP/6-31+G (d,p) level, the activation barrier of the concerted decarbonylation of ML (170 kJ mol^{-1}) is very close to that of the rate-determining step of the stepwise decarbonylation of ML (171 kJ mol^{-1}). As a consequence, decarbonylation of ML over the catalyst can be regarded as to proceed equally via both stepwise and concerted mechanisms.

3.3. Decomposition of ML to AA and methanol

Decomposition of ML to AA and methanol over the catalyst is also a stepwise mechanism which consists of four steps as shown in Fig. 4a and from Fig. 4d to f. In addition to the pathway of Fig. 4b which leads to the formation of AD and CO, the reaction intermediate P5 can also convert to R8 via releasing of a methanol molecule. This is an endothermic reaction with a reaction enthalpy of 65 (59) kJ mol^{-1}. R8 then undergoes two steps of isomerization as shown in Fig. 4d and e, forming reaction intermediates of P8

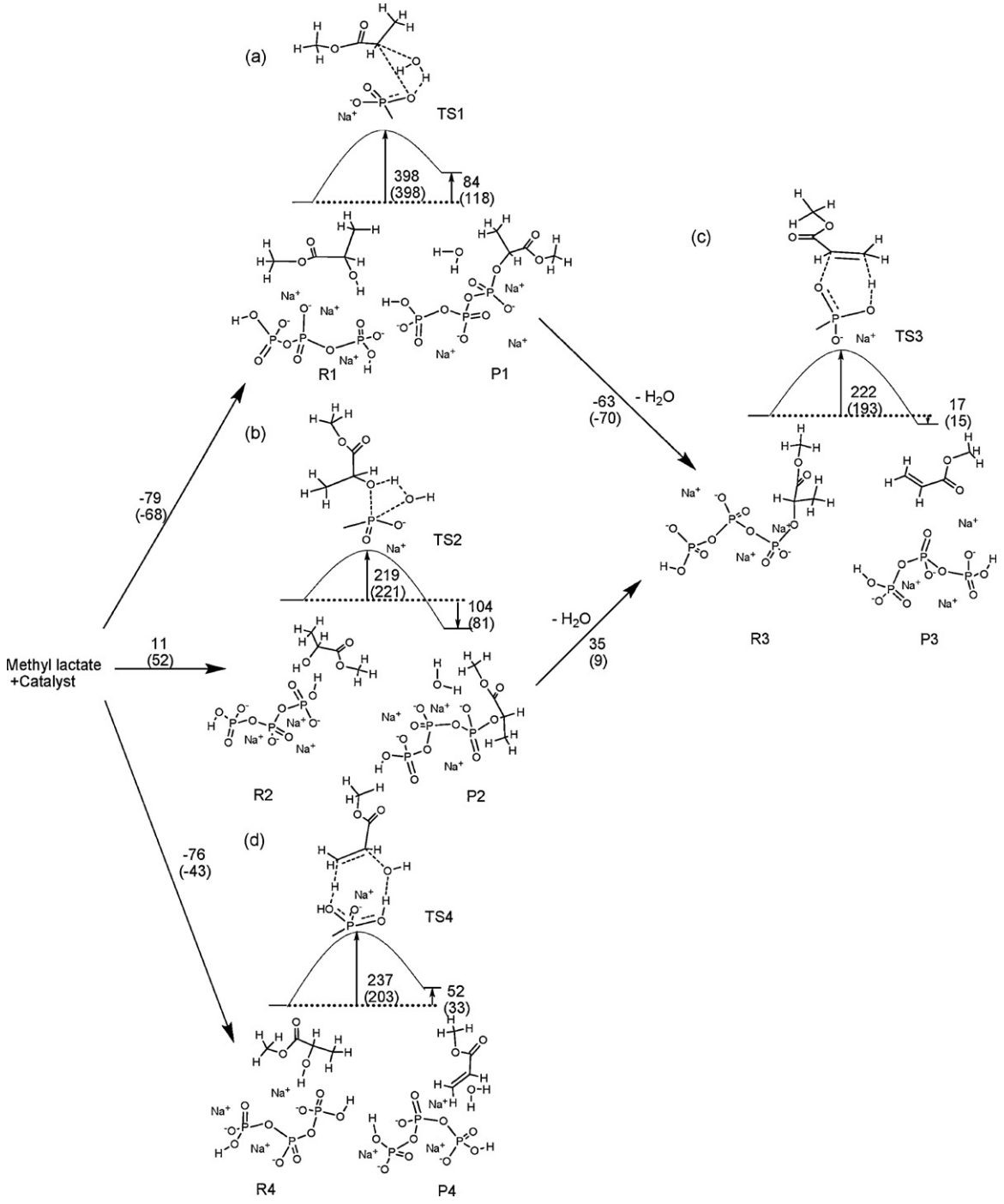

Fig. 3. Calculated energy diagrams of dehydration of ML over sodium tripolyphosphate. (a) and (b) The first step of stepwise dehydration; (c) the secondary step of stepwise dehydration; (d) concerted dehydration. (Energy scale in kJ mol^{-1}. The values in the parentheses were obtained at the B3LYP/6-31+G (d,p) level.)

and P9, respectively. Subsequently P9 undergoes a conformation change to R10, an intermediate for the formation of AA. In the first isomerization step, a proton is transferred from the hydroxyl group of ML to P═O, forming P8 with an activation barrier of 117 (112) kJ mol^{-1}. Vibrational frequency analysis for P8 indicated that there was no imaginary frequency and thus the structure was a stable local minimum. Due to the strained ring structure, the energy of P8 is higher than R8 and this step is an endothermic reaction with a reaction enthalpy of 77 (85) kJ mol^{-1}. P8 can undergo a conformation change to R9. This is an exothermic reaction with a reaction enthalpy of 35 (41) kJ mol^{-1}. Proton transfer from POH to the CO group and cleavage of the P–O bond lead to the formation of a phosphate ester P9 from R9, which has an activation barrier of only 36 (32) kJ mol^{-1} and is exothermic with a reaction enthalpy of 35 (39) kJ mol^{-1}. These mean that this step can easily take place. P9 then converts to R10 via a conformation change with an exothermic reaction enthalpy of 17 (13) kJ mol^{-1}. Finally, AA is formed from R10 via a proton transfer from the methyl group of ML to the P═O group of the catalyst and a cleavage of a C–O bond with an activation barrier of 142 (145) kJ mol^{-1}. From the values of activation barriers it is known that the rate-determining step for the decomposition of ML to MA and methanol is the first

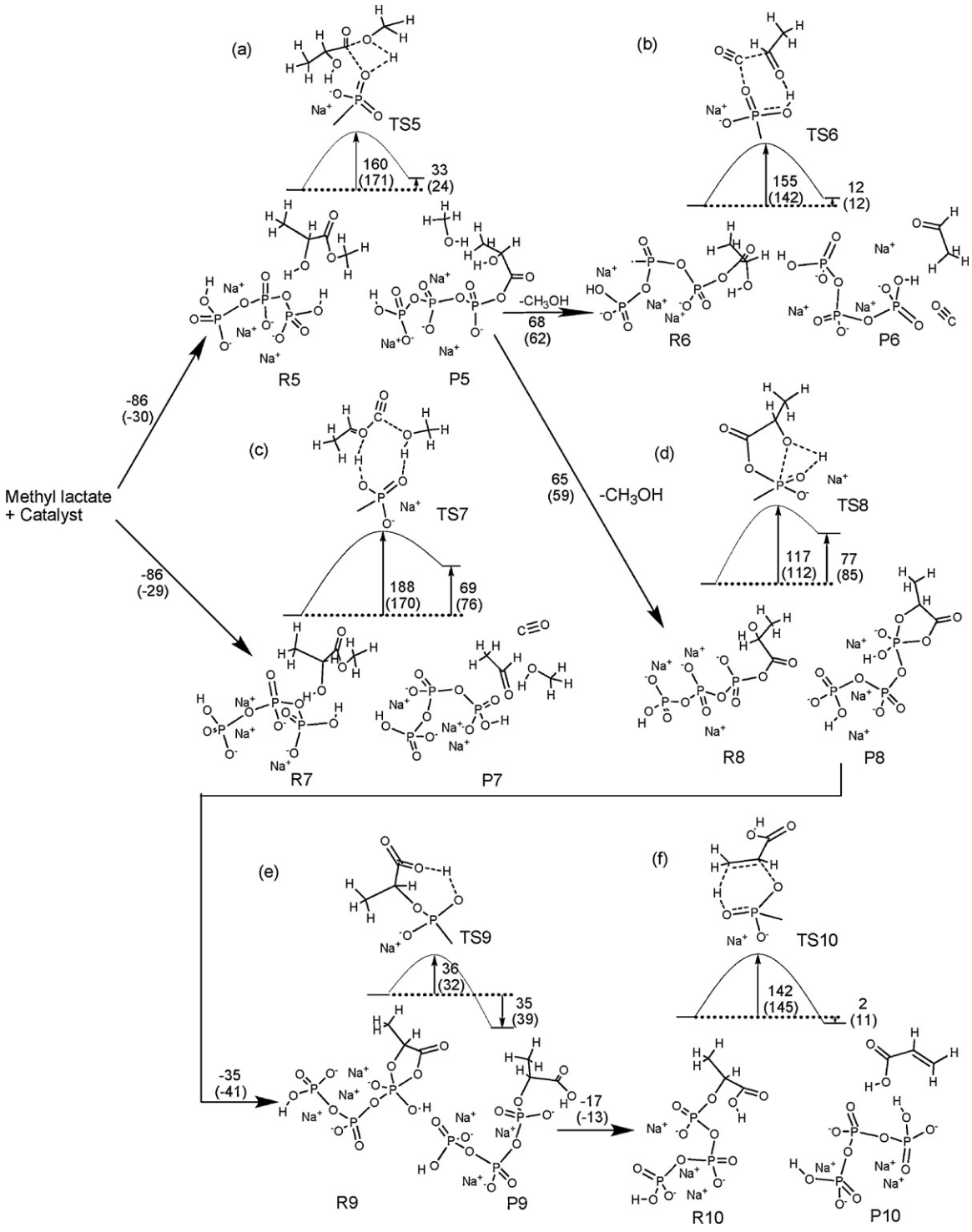

Fig. 4. Calculated energy diagrams of decarbonylation of ML and decomposition of ML to AA over sodium tripolyphosphate. (a) the first step of stepwise decarbonylation; (b) the secondary step of stepwise decarbonylation; (c) concerted decarbonylation; (d) the first step of proton transfer of phosphate ester; (e) the second step of proton transfer of phosphate ester; (f) decomposition of phosphate ester to AA. (Energy scale in kJ mol^{-1}. The values in the parentheses were obtained at the B3LYP/6-31+G (d,p) level.)

step (Fig. 4a). It can also noted that decomposition of ML to MA and decarbonylation of ML start from the same reaction intermediate (P5) and the activation barriers of the subsequent reaction steps favor the decomposition of ML to MA and methanol over the decarbonylation reaction at the MP2/6-31+G (d,p) level. While at the B3LYP/6-31+G (d,p) level, decarbonylation and decomposition probably occur equally.

3.4. Hydrolysis of ML and MA and esterification of LA and AA

It is known that the hydrolysis of esters and esterification of acids with alcohols can be accelerated by acidic catalysts [19,20]. Due to the presence of H_2O and methanol, hydrolysis of ML and MA and esterification of LA and AA catalyzed by the catalyst are all possible reactions in this system. Therefore, these two types of

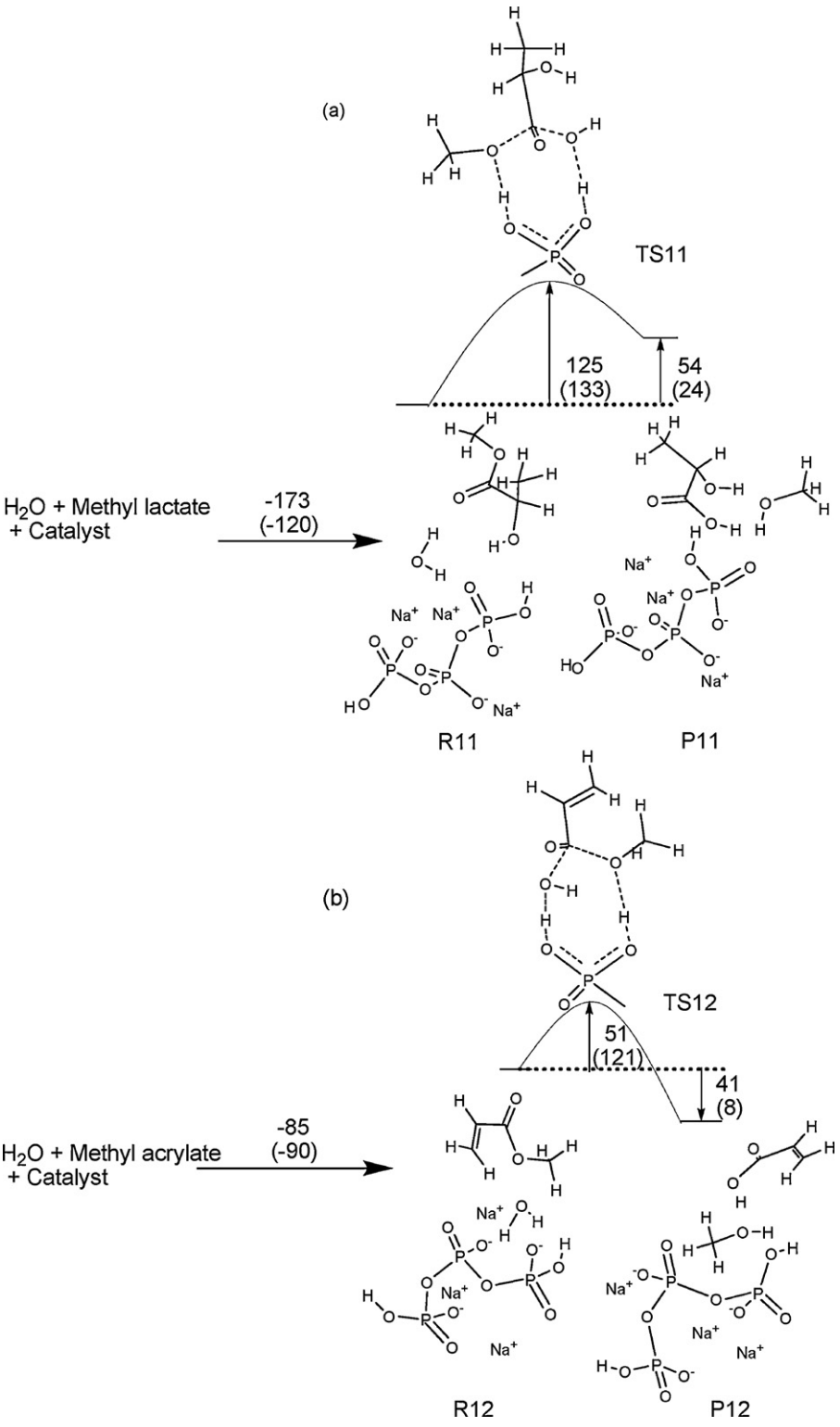

Fig. 5. Calculated energy diagrams of (a) hydrolysis of ML to LA and (b) hydrolysis of MA to AA over sodium tripolyphosphate. (Energy scale in kJ mol^{-1}. The values in the parentheses were obtained at the B3LYP/6-31+G (d,p) level.)

reactions were investigated and the reaction mechanisms are given in Fig. 5. Adsorption of ML and H_2O on the catalyst forms R11, which is an exothermic reaction with an enthalpy of 173 (120) kJ mol^{-1}, Conversion of R11 to P11 produces LA and methanol. This reaction has an activation barrier of 125 (133) kJ mol^{-1}. Adsorption of MA, H_2O on the catalyst leads to the formation of R12, which is also an exothermic reaction with an enthalpy of 85 (90) kJ mol^{-1}. The reaction barrier from R12 to P12, which leads to the hydrolysis of MA, is 51 (121) kJ mol^{-1}. The reverse reactions of the above two hydrolysis reactions are the esterification of LA and AA with methanol. The reaction barrier for the esterification of LA is 71 (109) kJ mol^{-1} and for the esterification of AA is 92 (129) kJ mol^{-1}.

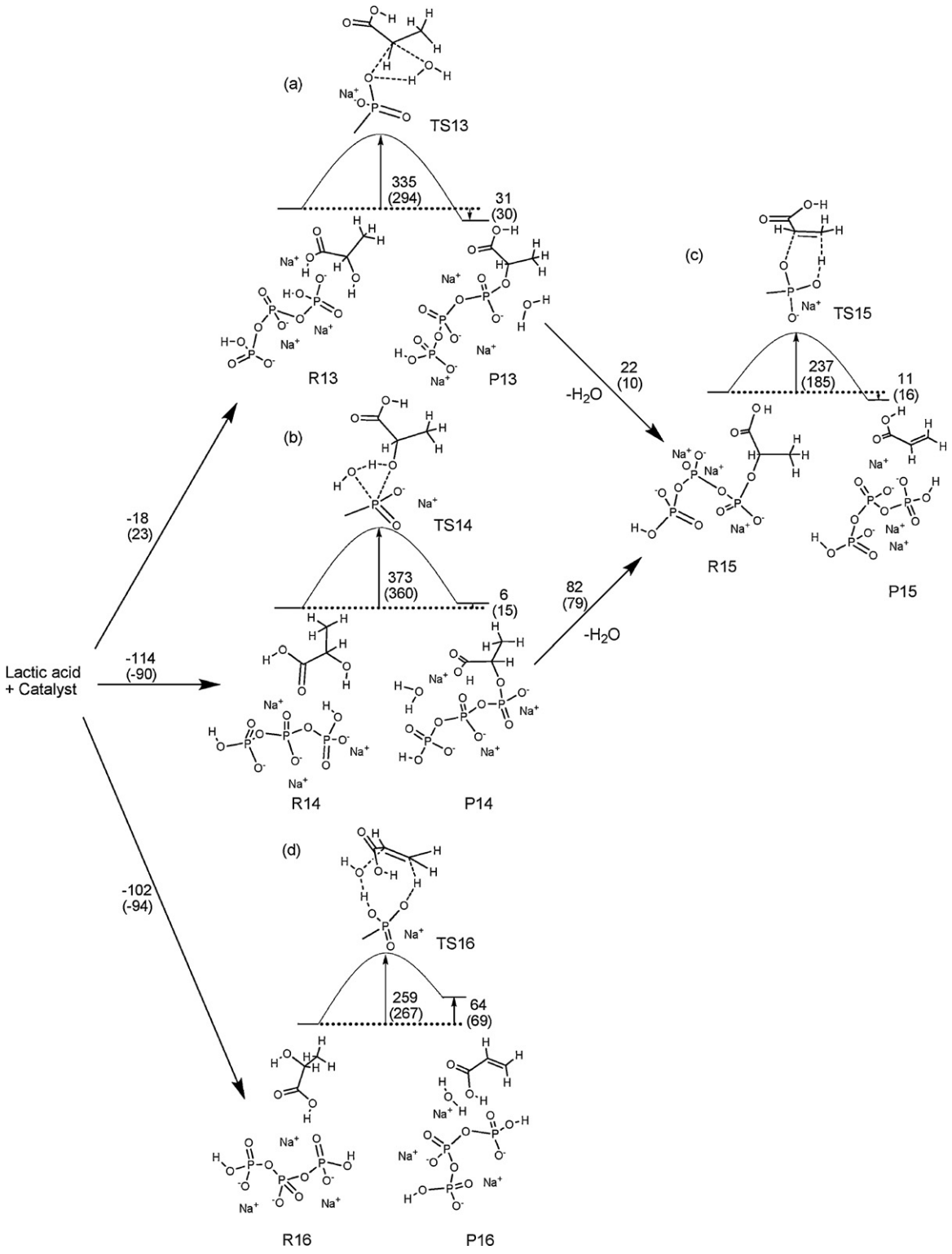

Fig. 6. Calculated energy diagrams of dehydration of LA over sodium tripolyphosphate. (a) and (b) The first step of the stepwise dehydration; (c) the secondary step of the stepwise dehydration; (d) the concerted dehydration (Energy scale in kJ mol^{-1}. The values in the parentheses were obtained at the B3LYP/6-31+G (d,p) level.)

3.5. Dehydration of LA

Over the catalyst dehydration of LA to AA and H_2O can also occur. The mechanisms of this reaction can be deduced similarly as for the dehydration of ML. Fig. 6a–c shows the stepwise dehydration of LA to AA and H_2O. The first step of the stepwise mechanisms is the formation of a phosphate ester via the pathways shown in Fig. 6a and b, respectively. In Fig. 6a the phosphate ester is formed by elimination of the proton of POH group of the catalyst and the hydroxyl of LA with an activation barrier of 335 (294) kJ mol^{-1} In Fig. 6b the phosphate ester is formed by elimination of the proton of LA and the hydroxyl of the POH group of the catalyst with an activation barrier of 373 (360) kJ mol^{-1}. The second step (Fig. 6c) is the formation of AA from the phosphate ester which has an activation

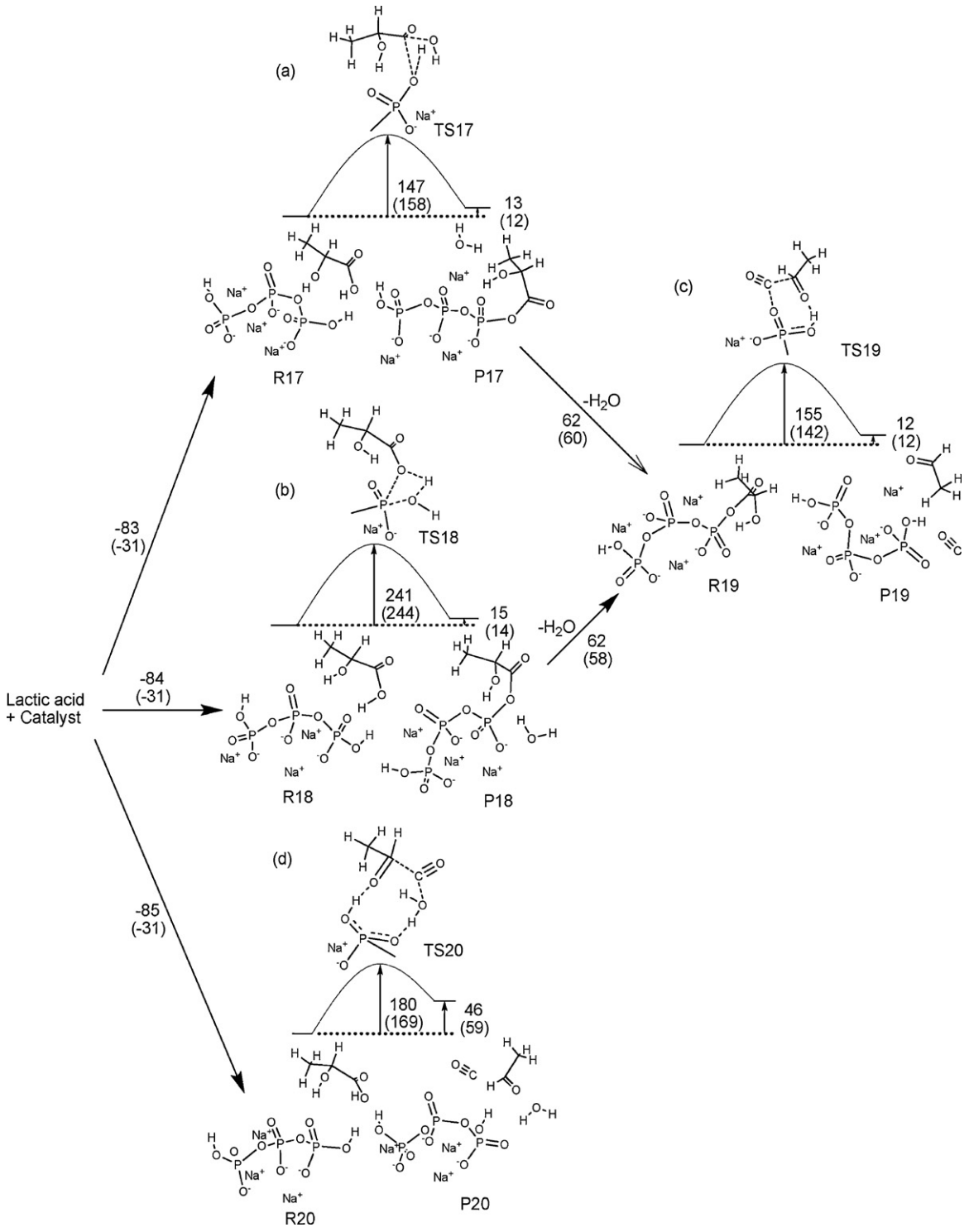

Fig. 7. Calculated energy diagrams of decarbonylation of LA over sodium tripolyphosphate. (a) and (b) the first step of stepwise decarbonylation; (c) the secondary step of stepwise decarbonylation; (d) the concerted decarbonylation. (Energy scale in kJ mol^{-1}. The values in the parentheses were obtained at the B3LYP/6-31+G (d,p) level.)

barrier of 237 (185) kJ mol^{-1}. Apparently, the first step of the stepwise mechanisms from LA to AA and H_2O is the rate-determining step. Fig. 6d is the concerted mechanism for the dehydration of LA to AA and H_2O. With this mechanism the reaction has an activation barrier of 259 (267) kJ mol^{-1}. The values of the activation barriers obtained for the dehydration of LA via different routes clearly indicate that the concerted mechanism is the dominant route.

3.6. Decarbonylation of LA

Fig. 7 shows the mechanisms of decarbonylation of LA to AD, CO and H_2O. Here two stepwise mechanisms and one concerted mechanism are proposed. The first steps of the stepwise mechanisms are the formation of a phosphate ester as shown in Fig. 7a and b. In Fig. 7a, the phosphate esters is produced via elimination of the hydroxyl group of LA and the proton of POH group of the

Table 1
Activation barriers of the predominant pathways of reactions (1)–(9).

Reaction	Mechanism	Activation barrier (kJ mol^{-1})	
		MP2	B3LYP
(1) Dehydration of ML	Stepwise	222	
	Concerted		203
(2) Decarbonylation of ML	Stepwise	160	171
	Concerted		170
(3) Decomposition of ML	Stepwise	160	171
(4) Hydrolysis of ML	Concerted	125	133
(5) Esterification of LA	Concerted	71	109
(6) Hydrolysis of MA	Concerted	51	121
(7) Esterification of AA	Concerted	92	129
(8) Dehydration of LA	Concerted	259	267
(9) Decarbonylation of LA	Stepwise	155	158

catalyst with an activation barrier of 147 (158) kJ mol^{-1}. In Fig. 7b, the phosphate ester is formed by elimination of the hydroxyl of the POH group of the catalyst and the proton of LA with an activation barrier of 241 (244) kJ mol^{-1}. In the second step, AD and CO are formed via decomposition of the phosphate ester with an activation barrier of 155 (142) kJ mol^{-1}. The concerted decarbonylation mechanism of LA is shown in Fig. 7d. The activation barrier of this pathway is 180 (169) kJ mol^{-1} The values of the activation barriers obtained for the decarbonylation of LA over the catalyst via the three different routs indicate that the first stepwise mechanism shown in Fig. 7a and c is the main route at both the MP2/6-31+G (d,p) as well as the B3LYP/6-31+G (d,p) levels. However, there is a slight difference. The MP2/6-31+G (d,p) method predicts the second step shown in Fig. 7c as the rate-determining step, while the B3LYP/6-31+G (d,p) method predicts the first step shown in Fig. 7a as the rate-determining step.

4. Discussion

The activation barriers of the predominant pathways of reactions (1)–(9) are summarized in Table 1.

Reactions (1)–(4) are those that ML directly converts to products. Reaction (4) has the lowest activation barrier as compared to reactions (1)–(3). However, the presence of its reverse reaction as well as the higher activation barrier as compared to that of reaction (5) make reaction (4) unlikely the main route for the consumption of ML. Direct dehydration of ML to MA through reaction (1) has an activation barrier of 222 (203) kJ mol^{-1}, which is about 62 (33, 32) kJ mol^{-1} higher than that of reactions (2) and (3). This implies that consumption of ML through dehydration route has a small possibility. Therefore, the main consumption routes of ML can be attributed to reactions (2) and (3). At MP2/6-31+G (d,p) level, reactions (2) and (3) both start from the same reaction intermediate P5. According to the activation barriers of the subsequent steps, formation of AA is favored over decarbonylation. The activation barriers obtained at the B3LYP/6-31+G (d,p) level indicate that both decomposition of ML to AA and methanol as well as decarbonylation of ML practically take place with equal probability.

As discussed above, the possibility for the formation of MA via the direct dehydration of ML is very small. However, there is always a significant amount of MA present in the reaction effluent [11,12]. The main route for the formation of MA is likely via the reaction between AA and methanol as shown in Fig. 6b. Upon the decomposition and decarbonylation of ML, AA and methanol are produced. Due to the presence of the catalyst, esterification of AA with methanol can take place. However, this reaction can only proceed to a certain extent since the activation barrier of its reverse reaction is higher. The existence of esterification of AA and hydrolysis of MA in the reaction system is supported by the experimental observations that under the similar reaction conditions, adding methanol to ML feed resulted in an increase in the selectivity to MA, while adding H_2O resulted in an increase in the selectivity to AA [11]. Based on the above discussion, it can be concluded that the predominant routes for the conversion of ML over the catalyst are the decomposition to AA and methanol and the decarbonylation to AD, Methanol and CO.

The product distribution of the conversion of ML over NaH_2PO_4/SiO_2 has been reported by Zhang et al. [11,12]. At 340 °C and a conversion of ML of 78.9%, the selectivity to methanol, AD, MA, AA, CO, CO_2 and unknown products (mainly products with boiling pints higher than LA) is 43.1%, 12.3%, 9.0% 30.8%, 17.2%, 1.6% and 30.2%. It can be noticed that even with ML as a feedstock about 30% of the converted ML is present as high boiling pint products. The experimentally observed selectivity ratio of (AA + MA) to AD is 3.2. Using the assumption of steady state for the steps from Fig. 4d to f, it can be found that the formation rate of AA from P5 is related not only to the rate coefficient of the step of Fig. 4f but also to the equilibrium constants of the steps of Fig. 4d and e. If it is supposed that the pre-exponential factors of the reactions shown in Fig. 4b and f have the same value, the calculated reaction rate ratio for the step of Fig. 4f to b at 340 °C using the activation barriers obtained at MP2/6-31+G (d,p) level is 12.8 without taking into account the equilibrium constants of the steps of Fig. 4d and e. The difference between the experimentally observed and the calculated selectivity ratio of (AA + MA) to AD may implies that the complicated reaction route for the decomposition of ML to AA and methanol is an important factor that hinders the formation of AA with high selectivity.

Dehydration of LA leads to the formation of AA and H_2O. On this catalyst, the calculated activation barrier is 259 (267) kJ mol^{-1}. This value is 104 (109) kJ mol^{-1} higher than that of the decarbonylation reaction of LA. This means that the predominant reaction of LA on the phosphate catalyst is decarbonylation.

Comparing the activation barriers for the formation of AA on the phosphate catalyst, it can be seen that conversion of ML to AA via reaction (3) has a significantly lower activation barrier than that of LA to AA via reaction (8). On the other hand, decarbonylation of ML and LA has comparable activation barriers. This means that using ML as a feedstock would obtain a higher yield of AA than using LA on the phosphate catalyst. Zhang [11] observed that with NaH_2PO_4/SiO_2 as a catalyst the highest selectivity from LA to AA is only 26%, supporting the calculated results.

Although the energetics estimated at the MP2/6-31+G (d,p) level show certain differences from that at the B3LYP/6-31+G (d,p) level, this does not have any influence for us to indentify the predominant consumption routes for the conversion of ML over the sodium polyphosphate catalyst. The reason can be attributed to the fact that most of the activation barriers of the concerned reactions are significantly different. The MP2 method gives more reasonable energetic values as it can predict results more consistent with the experimental observations.

5. Conclusions

A series of quantum chemical calculations with MP2 and B3LYP methods were carried out for probing the most possible reaction pathways of ML over sodium tripolyphosphate which was used as a model catalyst for sodium polyphosphate supported on silica. At both the MP2/6-31+G (d,p) and B3LYP/6-31+G (d,p) levels, the calculated results indicate that over the catalyst conversion of ML is mainly through the direct decomposition of ML to AA and methanol and the decarbonylation of ML to AD, methanol and CO. Both of them proceed via stepwise mechanisms and start from the

same reaction intermediate. In contrast, dehydration of ML to MA and H_2O is less important as compared to the above mentioned reactions. The main route for the formation of MA from ML is via esterification reaction of AA with methanol and this reaction can only proceed to a limited extent due to its higher activation barrier than that of the reverse reaction. Over the catalyst, the predominant consumption route for LA is decarbonylation, forming AD, H_2O and methanol. Therefore, using ML as a feedstock will obtain a higher selectivity to acrylate products than using LA.

Acknowledgment

This work was supported by the National Basic Research Program (973 Program, Grant No. 2007CB714304).

References

[1] L.A. Edye, W.O.S. Doherty, J.A. Blinco, G.E. Bullock, Int. Sugar J. 108 (2006) 19–27.
[2] R. Datta, M. Henry, J. Chem. Technol. Biotechnol. 81 (2006) 1119–1129.
[3] H. Danner, R. Braun, Chem. Soc. Rev. 28 (1999) 395–405.
[4] R.E. Holmen, Minnesota Mining & Manufacturing Company, US Patent 2,859,240 (1958).
[5] R.A. Sawicki, Texaco Inc., US Patent 4,729,978 (1988).
[6] J.F. Zhang, J.P. Lin, P.L. Cen, Can. J. Chem. Eng. 86 (2008) 1047–1053.
[7] J.F. Zhang, J.P. Lin, X.B. Xu, P.L. Cen, Chin. J. Chem. Eng. 16 (2008) 263–269.
[8] H.F. Shi, Y.C. Hu, Y. Wang, H. Huang, Chin. Chem. Lett. 18 (2007) 476–478.
[9] P. Sun, D. Yu, K. Fu, M. Gu, Y. Wang, H. Huang, H. Ying, Catal. Commun. 10 (2009) 1345–1349.
[10] H. Wang, D. Yu, P. Sun, J. Yan, Y. Wang, H. Huang, Catal. Commun. 9 (2008) 1799–1803.
[11] Z. Zhang, Ph.D. Thesis, Dehydration of methyl lactate and lactic acid to methyl acrylate and/or acrylic acid: a joint experimental and theoretical study, 2009.
[12] Z. Zhang, Y. Qu, S. Wang, J. Wang, Ind. Eng. Chem. Res. 48 (2009) 9083–9089.
[13] Gaussian 03, revision C02, Gaussian Inc., Pittsburgh, PA, 2004.
[14] C. Peng, P.Y. Ayala, H.B. Schlegel, M.J. Frisch, J. Comput. Chem. 17 (1996) 49–56.
[15] C. Peng, H.B. Schlegel, Israel J. Chem. 33 (1993) 449–454.
[16] C. Gonzalez, H.B. Schlegel, J. Phys. Chem. 94 (1990) 5523–5527.
[17] J.R.V. Wazer, K.A. Holst, J. Am. Chem. Soc. 72 (1950) 639–644.
[18] L.F. Nims, J. Am. Chem. Soc. 56 (1934) 1110–1112.
[19] M.-J. Lee, P.-L. Chou, H.-m. Lin, Ind. Eng. Chem. Res. 44 (2005) 725–732.
[20] M.T. Sanz, R. Murga, S. Beltran, J.L. Cabezas, J. Coca, Ind. Eng. Chem. Res. 43 (2004) 2049–2053.